

Cite this: *J. Anal. At. Spectrom.*, 2011, **26**, 565

www.rsc.org/jaas

PAPER

High-precision Mg-isotope measurements of terrestrial and extraterrestrial material by HR-MC-ICPMS—implications for the relative and absolute Mg-isotope composition of the bulk silicate Earth

Martin Bizzarro,* Chad Paton, Kirsten Larsen, Martin Schiller, Anne Trinquier and David Ulfbeck

Received 15th October 2010, Accepted 7th December 2010

DOI: 10.1039/c0ja00190b

We report novel methods for the chemical purification of Mg from silicate rocks by ion-exchange chromatography, and high-precision analysis of Mg-isotopes by high-resolution multiple collector inductively coupled plasma source mass spectrometry (HR-MC-ICPMS). Using these methods, we have measured the relative and absolute Mg-isotope composition of a number of terrestrial and extraterrestrial materials, including international reference rock standards as well as pure Mg standards, olivine crystals separated from a mantle-derived spinel lherzolite (J12 olivine), one enstatite chondrite, a martian shergottite and sea water samples. Repeated analyses of terrestrial and extraterrestrial samples demonstrate that it is possible to routinely measure the relative Mg-isotope composition of silicate materials with an external reproducibility of 2.5 and 20 ppm for the $\mu^{26}\text{Mg}^*$ and $\mu^{25}\text{Mg}$ values, respectively (μ notation is the per 10^6 deviation from a reference material). Analyses of bulk mantle-derived rocks as well as a martian shergottite and an enstatite chondrite define a restricted range in $\mu^{25}\text{Mg}$ of -120 ± 28 ppm (2sd) relative to the DSM-3 reference standard ($\mu^{25,26}\text{Mg} = 0$), suggesting that the Mg-isotope composition of inner solar system bulk planetary materials is uniform within the resolution of our analyses. We have determined the absolute Mg-isotope composition of the J12 olivine, two CI chondrites as well as the DSM-3 and Cambridge-1 reference standards using a mixed ^{26}Mg - ^{24}Mg double-spike. The differences between the absolute $^{25}\text{Mg}/^{24}\text{Mg}$ ratios of the various materials analyzed relative to the DSM-3 standard are in excellent agreement with results obtained by the sample-standard bracketing method. Based on the averages obtained for the J12 olivine separates, we estimate the absolute Mg-isotope composition for Earth's mantle – and hence that of the bulk silicate Earth – to be $^{25}\text{Mg}/^{24}\text{Mg} = 0.126896 \pm 0.000025$ and $^{26}\text{Mg}/^{24}\text{Mg} = 0.139652 \pm 0.000033$. Given the restricted range of $\mu^{25}\text{Mg}$ obtained for bulk planetary material by the sample-standard bracketing technique and the excellent agreement between the data obtained by the relative and absolute methods, we propose that these new values represent the absolute Mg-isotope composition of the bulk inner solar system. Using the absolute Mg-isotope composition of the J12 olivine, we calculate the isotopic abundances of Mg as $^{24}\text{Mg} = 0.789548 \pm 0.000026$, $^{25}\text{Mg} = 0.100190 \pm 0.000018$, and $^{26}\text{Mg} = 0.110261 \pm 0.000023$. Based on this result, we have calculated an atomic weight for Mg of 24.305565 ± 0.000045 , which is marginally heavier than previous estimates but a factor of 10 more precise.

1 Introduction

Magnesium is the sixth most abundant element in the sun,¹ and one of the most important rock-forming constituents of planets from the inner solar system. Magnesium has three naturally occurring isotopes - ^{24}Mg , ^{25}Mg and ^{26}Mg - with relative abundances of $\sim 79\%$, 10% and 11% , respectively. Variations in the isotopic composition of Mg can potentially occur in solar system

materials through a number of processes including (1) stellar nucleosynthesis, (2) the former presence and decay of the ^{26}Al nuclide (half-life = 0.73 myr) and (3) mass-dependent isotopic fractionation during high-temperature processes such as partial evaporation/condensation as well as from low-temperature fluid/rock interactions (*e.g.* aqueous alteration in carbonaceous chondrites). Thus, studying the potential variability of $^{26}\text{Mg}/^{24}\text{Mg}$ and $^{25}\text{Mg}/^{24}\text{Mg}$ ratios in solar system solids can be used to infer genetic relationships between early solar system reservoirs and terrestrial planets.

Until recently, Mg-isotope studies have largely focused on the search for the presence of live ^{26}Al in early solar system objects and

Centre for Star and Planet Formation, Natural History Museum of Denmark, University of Copenhagen, DK-1350 Copenhagen, Denmark. E-mail: bizzarro@snm.ku.dk

its use as a high-resolution early solar system chronometer,^{2–4} or on the detection of mass-independent anomalous effects.^{5,6} With the advent of multi-collector inductively coupled mass spectrometry (MC-ICP-MS), however, it is now possible to routinely measure Mg-isotopes with greatly improved precision compared to traditional techniques such as thermal ionization mass spectrometry (TIMS) or secondary ionization mass spectrometry (SIMS). For example, building on the pioneering work of Galy *et al.*,⁷ most recent Mg-isotope studies of silicate materials by solution mode MC-ICPMS report the ²⁵Mg/²⁴Mg ratio with a typical analytical uncertainty of ~100 ppm.^{8–13} Yet, despite this significant improvement in precision, the Mg isotopic composition of Earth remains poorly constrained, a critical consideration for the full use of ²⁵Mg/²⁴Mg and ²⁶Mg/²⁴Mg ratios as tracers of planet-forming processes.

The ability to determine the Mg-isotope composition of minute meteoritic inclusions to high-precision by either solution mode or laser ablation MC-ICPMS has recently provided important insights into our understanding of the earliest evolution of the solar system, through the use of the ²⁶Al-²⁶Mg short-lived chronometer.^{14–19} The magnitude of the excess ²⁶Mg resulting from the *in situ* decay of ²⁶Al (²⁶Mg*) can routinely be measured with a precision of 20–30 ppm for the oldest solar system solids such as calcium-aluminium refractory inclusions (CAIs), translating into age uncertainties of less than 50,000 years when calculating model ages for the formation of these objects.^{15,18,19} A central assumption in the use of the ²⁶Al-²⁶Mg system as a robust chronometer is the homogeneity of the parent ²⁶Al nuclides within inner solar system materials. Although some recent studies have inferred a homogeneous distribution of ²⁶Al based on either the Mg-isotope measurements of inner solar system solids¹⁸ or, alternatively, concordancy between ²⁶Al-²⁶Mg and Pb–Pb ages of chondritic components,^{20,21} we note that the resolution required to unequivocally ruled-out ²⁶Al heterogeneity is beyond the current state-of-the-art in Mg-isotope measurements. For example, accepting the initial ²⁶Al/²⁷Al ratio [²⁶Al/²⁷Al]₀ of 5.23×10^{-5} (ref. 19), the amount of radiogenic ²⁶Mg resulting from the *in situ* decay of ²⁶Al (²⁶Mg*) in a reservoir with solar ²⁷Al/²⁴Mg ratio of 0.101 is only 38 parts per million (ppm). As a result, an uncertainty of ±10 ppm in measurements of the μ²⁶Mg* value in whole-rock samples of meteorites with an approximately solar ²⁷Al/²⁴Mg ratio could conceal a heterogeneity of up to 50% in [²⁶Al/²⁷Al]₀, which would clearly compromise the chronological significance of the ²⁶Al-²⁶Mg clock. Moreover, the recent discovery of variable U-isotope compositions of early solar system solids²² cast doubts on the accuracy of ²⁰⁷Pb-²⁰⁶Pb ages used to infer consistency with the ²⁶Al-²⁶Mg clock.

Given these caveats, we have developed novel analytical protocols allowing the measurement of both relative and absolute Mg-isotope ratios to unprecedented precision and accuracy. In detail, we provide mass spectrometry and chemical purification techniques that allow for measurement of the ²⁶Mg*, relative ²⁵Mg/²⁴Mg and absolute ²⁵Mg/²⁴Mg and ²⁶Mg/²⁴Mg values in silicate materials with an external reproducibility of 2.5, 20, 195 and 235 ppm, respectively. Using these methods, we have determined the Mg-isotope composition of a number of international reference materials relative to the DSM-3 Mg standard,²⁰ as well as the absolute Mg-isotope composition of the

DSM-3 and Cambridge-1 synthetic standard solutions, the J12 olivine, and two CI carbonaceous chondrites using a ²⁶Mg-²⁴Mg double-spike.

2 Analytical procedures

2.1 Material analyzed and sample digestion

A variety of terrestrial and extraterrestrial materials were selected for analysis in this study. Five terrestrial international standard reference materials were chosen: BHVO-2 (Hawaiian basalt), BIR-1 (Iceland basalt), and DTS-2 (dunite), all obtained from the United States Geological Survey (USGS), as well as mid and north Atlantic sea water standards obtained from OSIL (Ocean Scientific International Limited). We have also analyzed olivine crystals separated from a spinel lherzolite from Yemen (J12 olivine; Shaw *et al.*)²³ as well as the Alais and Orgueil CI carbonaceous chondrites, the SAH 97159 enstatite chondrite, and the NWA 856 martian shergottite. All extraterrestrial materials were obtained from Labenne Meteorites. We have also analyzed a number of synthetic standard Mg solutions, including the DSM-3 and Cambridge-1 standards.²⁴

Apart for DTS-2, approximately 2–5 mg of rock powder from the international rock standards was weighed and digested in Savillex beakers with concentrated HF-HNO₃ mixtures on a hotplate at 130 °C. To ensure complete dissolution of more refractory phases such as chromite present in DTS-2, and aliquot of *ca.* 25 mg was digested in a Parr bomb at 210 °C. A small fragment (<5 mg) was broken-off the main mass of the NWA 856 martian meteorite and then powdered in a boron carbide mortar before HF-HNO₃ digestion in Savillex beakers. Larger fragments were selected for the chondrite meteorites, namely 10, 10 and 20 mg for the Alais, Orgueil and SAH 97159 chondrites, respectively. These were digested in Parr bombs at 210 °C to ensure complete dissolution of potential refractory components. Approximately 0.2 mL of the seawater standards were dried down, fluxed for 12 h at 110 °C in 1 mL of *aqua regia* and evaporated to dryness and then converted to chloride form.

2.2 Mg purification

Following digestion, samples were evaporated to dryness and redissolved in 6M HCl to ensure complete dissolution. Chemical purification of Mg was achieved in a six steps procedure inspired by a number of previous studies,^{25–28} and following a modified version of the technique reported by Schiller *et al.*²⁹ as summarized in Table 1 and described in detail below:

1. Following dry down from the initial dissolution procedure, the sample was dissolved in 0.5 mL of 6M HCl and passed through a 1.25 mL pipette tip column loaded with 0.5 mL AG 1-X8 200–400 mesh anion exchange resin. Mg was eluted from the column with 2 mL of 6M HCl while Fe was retained on the column.

2. After dry down, the Mg cut from the first step was redissolved in 0.5 mL of 0.5M HCl and loaded on a cation exchange column containing 1 mL of Biorad AG50W-X8 200–400 mesh resin. Na and Cr were eluted with 3 mL of 0.5M HCl followed by 4 mL of 1M HNO₃, whereas Al and Ti were eluted with 2 mL of 2M HF. Magnesium was collected from the column with 8 mL of 6M HCl.

Table 1 Six steps Mg purification scheme

Eluent	Vol. ^a	Elements eluted
Step 1: Fe clean-up^b		
6M HCl	2	Conditioning
Load sample in 6M HCl	0.5	
6M HCl	2	Mg + matrix
Step 2: Cr, Na, Al, Ti clean-up^c		
0.5M HCl	3	Conditioning
Load sample in 0.5M HCl	0.5	
0.5M HCl	3	Cr + Na
1M HNO ₃	4	Cr + Na
2M HF	2	Al + Ti
6M HCl	8	Mg + Ca, Mn, Ni
Step 3: Ca clean-up^d		
3M HNO ₃	3	Conditioning
Load sample in 3M HNO ₃	1	
3M HNO ₃	4	Mg + Mn, Ni
Step 4: Mn clean-up^e		
0.5M HCl-95% acetone	3	Conditioning
Load sample in 0.5M HCl-95% acetone	2	
0.5M HCl-95% acetone	4	Mn
6M HCl	8	Mg + Ni
Step 5: Ni clean-up^f		
~0.2M NH ₄ OH + 0.1M HCl	3	Conditioning
Load in ~0.2M NH ₄ OH + 0.1M HCl	2	
~0.2M NH ₄ OH + 0.1M HCl	4	Mg
Step 6: Na clean-up^g		
0.5M HCl	3	Conditioning
Load sample in 0.5M HCl	0.5	
0.5M HCl	7	Na
6M HCl	8	Mg

^a Volume of eluent (mL). ^b 1.5 mL pipette tip column with 0.5 mL AG 1X8 200–400 mesh resin. ^c Biorad-type column with 1 mL of Biorad AG50W-X8 200–400 mesh resin. ^d Biorad-type column with 1 mL of TODGA resin. ^e Biorad-type column with 1 mL of BioRad AG50W-X8 200–400 mesh resin. ^f Biorad-type column with 1 mL of Eichrom Ni-spec resin. ^g Biorad-type column with 1 mL of Biorad AG50W-X8 200–400 mesh resin. New pre-cleaned resins were used in all steps.

3. The Mg cut from the second step was dried down, converted in chloride form, redissolved in 1 mL of 3M HNO₃ and loaded on a column containing 1 ml of diglycolamide resin (TODGA).³⁰ Magnesium was eluted from the column with 4 mL of 3M HNO₃, while Ca was retained on the diglycolamide resin.

4. The Mg cut from the third step was dissolved in 2 mL of 0.5M HCl-95% acetone and loaded on a column containing 1 mL of BioRad AG50W-X8 200–400 mesh resin. Mn is not retained on the resin in this acid molarity and high acetone concentration, which allows the elution of Mn from Mg in 4 mL of 0.5M HCl-95% acetone. Mg was collected from the column in 8 mL of 6M HCl.

5. After dry down, the Mg cut from the fourth step was dissolved in 1 mL of 0.1M HCl. Approximately 2.5 mL of >18.2 MΩ Millipore water and 0.5 mL of concentrated NH₄OH was added to the 0.1M HCl solution, resulting in a final solution with pH of 9–10. This solution was loaded onto a column containing 1 mL of Eichrom Ni-spec resin and the Mg was eluted from the column with an additional 4 mL of ~0.2M NH₄OH + 1M HCl solution adjusted to a pH >10. This solution was evaporated to

dryness, fluxed for 12 h at 110 °C in 1 mL of aqua regia, then evaporated to dryness again before conversion to chloride form.

6. The last step ensures removal of any Na that may have been introduced as blank during the previous steps. The Mg cut from the fifth step is dissolved in 1 mL of 0.5M HCl and loaded on a column containing 1 mL of Biorad AG50W-X8 200–400 mesh resin. The Na is eluted with 7 mL of 0.5M HCl, and the Mg is recovered with 10 mL of 6M HCl. Following dry down, the Mg cut is converted to nitrate form and ready for analysis on the mass spectrometer.

Although time consuming, the Mg purification scheme presented here ensures 99.9% recovery and excellent separation of Mg from elements that may create direct isobaric interferences (e.g. ⁴⁸Ca²⁺, ⁴⁸Ti²⁺, ⁵⁰Ti²⁺, ⁵⁰V²⁺, ⁵⁰Cr²⁺ and ⁵²Cr²⁺) and/or affect the instrumental mass discrimination as compared to the standard during analysis^{7,29} (e.g. Al, Fe, Na, Ni and Ca), as compared to previous studies typically based on a single cation-exchange chemistry.^{8–19} Moreover, it allows for the quantitative recovery of Fe, Cr, Ca and Ni thereby allowing for concurrent isotope analyses of these elements. Typical Al/Mg, Fe/Mg, Na/Mg, Ca/Mg, Ti/Mg, V/Mg, Ni/Mg and Cr/Mg ratios observed in the separated Mg fraction were <0.0001 and have negligible effects on the quality of our data. Total procedural blanks were <15 ng and negligible compared to the typical amount of Mg processed through the purification protocol (~200 µg).

2.3 Relative Mg-isotope measurements by HR-MC-ICPMS

Mg-isotopes were measured using the ThermoFisher Neptune MC-ICPMS located at the Centre for Star and Planet Formation, Natural History Museum of Denmark, University of Copenhagen. Following Mg purification, samples were converted to nitrate form, dissolved in a 2% HNO₃ solution and introduced into the plasma source by means of the ThermoFisher stable introduction system (SIS, wet plasma) or, alternatively, an Aridus II desolvating nebulizer (dry plasma). Typical sample aspiration rate using either of these introduction systems was approximately 0.060 mL min⁻¹. Magnesium isotope data were acquired in static mode using three Faraday collectors set-up as follows: ²⁶Mg in the high-3 collector on the high mass side of the axial Faraday, ²⁵Mg in the axial collector and, ²⁴Mg in the low-3 collector on the low mass side of the axial Faraday. The low-3 collector Faraday cup (²⁴Mg) was connected to an amplifier with a 10¹⁰ Ω feedback resistor, whereas the axial and high-3 collectors were connected to amplifiers with 10¹¹ Ω feedback resistors. Measurements were made in medium resolution mode (M/ΔM ~5000 as defined by the peak edge width from 5–95% full peak height) to resolve potential molecular interferences on the high-mass side (e.g. C₂⁺, C₂H⁺, C₂H₂⁺, CN⁺ and NaH⁺). Prior to each analytical session, we measured ²⁵Mg/²⁴Mg and ²⁶Mg/²⁴Mg ratios at different positions on the low-mass side of the Mg peak to define a flat plateau of ~100 ppm in width. Mg-isotope data were acquired at the center of this plateau, typically located ~0.012 a.m.u. from the center of the Mg peak. This position corresponds to an effective mass resolving power of ~2500, enabling the full resolution of all molecular interferences on the high mass side apart from ²⁴MgH⁺, which is only resolved at the 70% level. The hydride production under these analytical conditions is typically <100 ppm for Mg. The sensitivity of the instrument under these

analytical conditions was typically 20V/ppm and 100V/ppm Mg using the SIS and Aridus introduction systems, respectively. Samples and standards were analyzed with a signal intensity of at least 100V on mass ^{24}Mg , translating in a concentration of ~ 5 ppm when solutions introduced into the plasma source through the SIS. Each analysis comprised a total of 630 s of baseline measurements (obtained in defocus mode) and 1667 s of data acquisition (100 scans integrated over 16.67 s). Sample analyses were interspaced by analyses of the DSM-3 standard²⁴ to monitor instrumental mass fractionation, and each sample was systematically analyzed 10 times. This corresponds to a total of ~ 200 μg Mg consumed for each sample. A rinse time of 8 min was applied between sample and standard analyses.

2.4 Absolute Mg-isotope measurements by HR-MC-ICPMS

To determine the absolute isotopic composition of Mg, we employed a double-spike method using an approximately equal mixture of highly purified ^{24}Mg and ^{26}Mg , where the ratio of the two isotopes was gravimetrically determined to high-precision. Conventional double-spike methods require four isotopes of the element of interest,^{31–33} so a modified method necessitating stability in the instrumental mass fractionation was developed, a characteristic that is readily achievable using the Neptune MC-ICPMS. Approximately 20 μg of purified Mg was dissolved in 10 ml of 2% HNO_3 to create a solution containing 2 ppm total Mg, then split into two portions. A double-spike solution of the same total Mg concentration (2 ppm) was added to one of these splits to create an approximately 60 : 40 mixture of sample and spike, without changing the concentration of Mg in the solution. The spiked and unspiked splits were then analyzed one after the other ten times, for all isotopes of Mg. Magnesium isotope data were acquired in static mode using three Faraday collectors set-up as follows: ^{26}Mg in the high-1 collector on the high mass side of the axial Faraday, ^{25}Mg in the axial collector, and ^{24}Mg in the low-3 collector on the low mass side of the axial Faraday. All Faraday cups were connected to amplifiers with 10^{11} Ω feedback resistors using amplifier rotation, and were calibrated for gain prior to each session. Measurements were made in high-resolution mode ($M/\Delta M > 7500$ as defined by the peak edge width from 5–95% full peak height) to resolve the potential molecular interferences listed above, plus $^{24,25}\text{MgH}^+$. Each analysis comprised a total of 150 s baseline measurements obtained on-peak, and 400 s of data acquisition (200 scans, each integrated over 2 s). A rinse time of 12 min was applied between analyses. All analyses containing spike were conducted using a separate sample and skimmer (X-cone) cone, SIS introduction system and nebuliser to the normal Mg-isotope method.

By bracketing spiked and unspiked aliquots of the sample and interpolating mass discrimination between analyses, it is possible to deconvolve both the amount of double-spike added and the absolute magnitude of the mass discrimination affecting results. To deconvolve these factors and resolve the absolute isotopic composition of the spike-free aliquot, we adopted an iterative data reduction approach. As a starting point, mass discrimination was estimated using the observed offset between the unspiked $^{26}\text{Mg}/^{24}\text{Mg}$ ratio and an initial guess for the ratio of 0.13982 (ref. 34). Mass discrimination corrected $^{25}\text{Mg}/^{24}\text{Mg}$ and $^{26}\text{Mg}/^{24}\text{Mg}$ ratios of the spiked and unspiked aliquots were then

calculated using the derived mass discrimination. The corrected ratios of the spiked and unspiked aliquots can then be combined to calculate the proportion of double-spike added to the sample using the following equation:

$$F = \frac{\left(\frac{^{26}\text{Mg}/^{25}\text{Mg}}{^{26}\text{Mg}/^{25}\text{Mg}}\right)_{\text{mix}} - \left(\frac{^{26}\text{Mg}/^{25}\text{Mg}}{^{26}\text{Mg}/^{25}\text{Mg}}\right)_{\text{sample}}}{\left(\frac{^{26}\text{Mg}/^{25}\text{Mg}}{^{26}\text{Mg}/^{25}\text{Mg}}\right)_{\text{spike}} - \left(\frac{^{26}\text{Mg}/^{25}\text{Mg}}{^{26}\text{Mg}/^{25}\text{Mg}}\right)_{\text{sample}}} \quad (1)$$

Where F = fraction of spike in mixture, mix = the spiked sample aliquot, $sample$ = the unspiked sample aliquot and $spike$ = the pure double-spike composition. Finally, using the derived proportion of spike added, the mass discrimination can be recalculated using the $^{25}\text{Mg}/^{24}\text{Mg}$ ratio of the spiked aliquot. The initial guess for mass discrimination is then adjusted accordingly, and the loop repeated until the results converge to within 1×10^{-10} .

2.5 Preparation of the ^{24}Mg - ^{26}Mg spike

The ^{24}Mg - ^{26}Mg double-spike was prepared gravimetrically from pure metals. Isotopically enriched Mg metal ($^{24}\text{Mg} > 99.9\%$ and $^{26}\text{Mg} > 99.4\%$) was obtained from the Oak Ridge National Laboratory (USA). Double-distilled ultra-pure water and double-distilled acids were used for the dissolution and dilution of spike solutions, with all work being conducted in laminar-flow clean hoods. Isotopically enriched Mg metals were prepared in a separate clean laboratory to normal samples, and a separate clean hood was used for the spiking of samples prior to mass spectrometry. Mg metals were dissolved in cold 0.5M HNO_3 , and separate pieces of each pure metal weighing a minimum of 1 mg were dissolved for stable Mg-isotope and trace element analyses.

The accuracy of the spike solutions and, thus, the double-spike method, is constrained by a combination of uncertainties in the absolute weights, purities, and isotopic compositions of each purified isotope. In order to obtain highly accurate weights, approximately 100 mg of each isotopically enriched Mg metal was used. Weighing of metals was conducted at *Dansk Fundamental Metrologi* (Denmark) and certified to the E2 level. The ^{24}Mg and ^{26}Mg metals used in the double-spike weighed 100.0473 ± 0.0010 mg and 99.3593 ± 0.0010 mg, respectively. Impurities in the isotopically enriched Mg metals were measured by Oak Ridge National Laboratory using spark source mass spectrometry. The quality of these assays varies dramatically, with detection limits of the ^{26}Mg metal of ~ 0.5 ppm, compared with detection limits of up to 1000 ppm for the ^{24}Mg metal. Given that the metals were all prepared in the same laboratory using identical methods, it is likely that their impurity levels are actually very similar, and are at the levels of the most sensitive assay. To verify this, 2 ppm solutions of each Mg spike were measured by ion counter on the Neptune MC-ICPMS. The ^{26}Mg metal assay impurities sum to 169 ppm, with the majority of impurities due to 12 main elements. We measured each of these elements in the pure metal solutions and found that the summed impurities of the ^{24}Mg and ^{26}Mg metals are within 10%. Conveniently, when considering the double-spike, impurities in the ^{24}Mg and ^{26}Mg metals cancel each other out, meaning that it is only the difference in the total impurities between these two metals that will affect the $^{26}\text{Mg}/^{24}\text{Mg}$ ratio of the double-spike and thus the accuracy of results. Here, we

conservatively estimate this difference as a maximum of 100 ppm of impurities, which directly equates to an uncertainty of 100 ppm in the $^{26}\text{Mg}/^{24}\text{Mg}$ ratio of the double-spike.

For such high accuracy weights, it is also necessary to consider the effects of oxidation of the metal surface, which will cause an overestimation of the mass of Mg. We estimate the oxide layer on Mg metal to be less than 2 nm when stored in dry air at room temperatures.³⁵ The isotopically enriched Mg metals were received as a thin metal plate, and therefore had large surface area to volume ratios. With dimensions of $1 \times 5 \times 10$ mm, a 2 nm surface layer equates to approximately 0.0005% (*i.e.* 5 ppm) of the total volume. If this layer is pure MgO it can be expected to be approximately 1.67 times heavier than pure Mg metal and thus cause an overestimation of the mass of atomic Mg by 0.00033% (3.3 ppm).

For the purified ^{24}Mg metal, the isotopic composition determined by Oak Ridge National Laboratories was used, which has an uncertainty on the main isotope of 200 ppm, but for the ^{26}Mg metal we were able to determine its isotopic composition using a standard-bracketing approach on the Neptune. Although the ability to correct for mass discrimination using this approach is somewhat limited, the extremity of the isotopic ratios means that the actual impact of mass discrimination uncertainties on determining isotopic abundances is minimal. Assuming a maximum drift in mass discrimination over 18 h of ± 2000 ppm on the $^{25}\text{Mg}/^{24}\text{Mg}$ ratio (a factor of 5 more than we ever observe over such a period) we were able to determine the isotopic abundances of the ^{26}Mg metal to better than 25 ppm.

Finally, absolute ratio determination is affected by the law used to correct mass discrimination, and is thus limited by how well the nature of instrumental fractionation can be constrained. As discussed in Section 3.2, we observe that drift within a session always occurs along a fractionation curve with an exponent (β) within the range of 0.499 to 0.501 (Fig. 1). We have therefore conservatively estimated the uncertainty the β to be 0.500 ± 0.0015 , which results in an uncertainty on absolute $^{25}\text{Mg}/^{24}\text{Mg}$ and $^{26}\text{Mg}/^{24}\text{Mg}$ ratios of 152 and 2 ppm, respectively (note that because we use a $^{26}\text{Mg}/^{24}\text{Mg}$ spike, variations in the mass discrimination law have virtually no impact on calculated $^{26}\text{Mg}/^{24}\text{Mg}$ ratios).

The uncertainties related to weighing errors, impurities, isotopic composition, oxidation and mass discrimination are all systematic errors, and do not need to be included when directly comparing the Mg-isotope ratios of different samples (*e.g.* Cambridge-1 relative to DSM-3). However, if the absolute Mg-isotope ratio is of importance then these systematic uncertainties must be included. When combined in quadrature, the sources of systematic error in the ^{24}Mg - ^{26}Mg double-spike and the analytical reproducibility amount to total uncertainties in measured absolute $^{25}\text{Mg}/^{24}\text{Mg}$ and $^{26}\text{Mg}/^{24}\text{Mg}$ ratios of 195 ppm and 235 ppm, respectively.

2.6 Data reduction

All data reduction was conducted off-line using the freely distributed Iolite data reduction package which runs within Igor Pro; the reader is referred to Hellstrom *et al.*³⁶ and the Iolite website (<http://iolite.earthsci.unimelb.edu.au/>) for further details. The data reduction modules used for Mg-isotope ratio

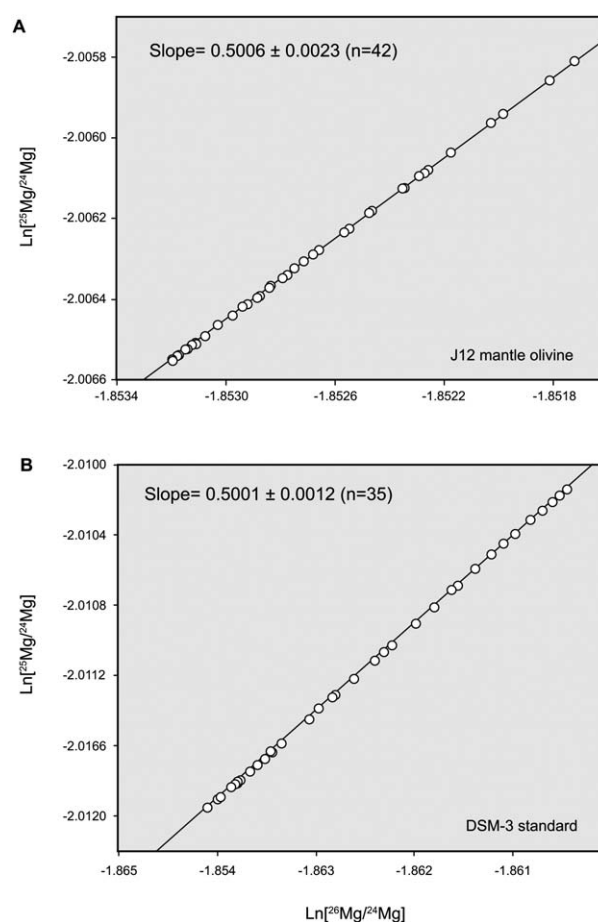


Fig. 1 Magnesium three isotope diagrams. Plotted are the natural logarithms of the raw $^{25}\text{Mg}/^{24}\text{Mg}$ and $^{26}\text{Mg}/^{24}\text{Mg}$ ratios obtained in two different analytical sessions for the J12 mantle olivine (A) and the DSM-3 pure Mg standard solution (B). Each point corresponds to 1667 s of data acquisition, and individual sessions were at least 35 h. Errors are smaller than symbols in all cases. Note that the slope ($= \beta$, ref. 55) of these mass fractionation lines is in best agreement a slope of 0.500.

calculations are freely available and can be obtained from the authors on request. Background intensities were interpolated using a smoothed cubic spline, as were changes in mass and elemental bias with time. Iolite's *Smooth spline auto* choice was used in all cases, which determines a theoretically optimal degree of smoothing based on variability in the reference standard throughout an analytical session, which corresponds typically to 36 to 60 h of continuous measurement without adjusting the instrument's tuning parameters when acquiring data for high-precision Mg-isotope determination. For each analysis the mean and standard error of the measured ratios were calculated, using a 3 sd threshold to reject outliers. Sample analyses were combined ($n = 10$) to produce an average weighted by the propagated uncertainties of individual analyses. Stable Mg-isotope ratios are reported as relative deviations from the DSM-3 Mg reference material²⁴ in the μ notation according to the following formula:

$$\mu^x\text{Mg} = \left[\frac{({}^x\text{Mg}/^{24}\text{Mg})_{\text{sample}}}{({}^x\text{Mg}/^{24}\text{Mg})_{\text{DSM-3}}} - 1 \right] \times 10^6 \quad (2)$$

Where $x = 25$ or 26 . We use the μ notation (per 10^6 deviations) instead of the traditional δ notation (per 10^3 deviations) for convenience given that the reproducibility and accuracy of the measurements obtained in this study are at the ppm level. The mass independent component in ^{26}Mg ($\mu^{26}\text{Mg}^*$) is reported in the same fashion, but represents deviations from the internally normalized $^{26}\text{Mg}/^{24}\text{Mg}$ of the sample from the reference standard, normalized to $^{25}\text{Mg}/^{24}\text{Mg} = 0.126896$ (see section 3.6) using the exponential mass fractionation law. This approach yields identical results to calculating the mass independent component in ^{26}Mg from the difference between the observed and predicted $\mu^{26}\text{Mg}$ based on the $\mu^{25}\text{Mg}$ assuming that natural fractionation of the sample is driven by a kinetic law according to the following equation:

$$\mu^{26}\text{Mg}^* = \mu^{26}\text{Mg} - \frac{\mu^{25}\text{Mg}}{0.511} \quad (3)$$

Young and Galy³⁷ introduced the $\Delta^{25}\text{Mg}'$ notation to facilitate the analysis of fractionation laws, where the $\Delta^{25}\text{Mg}'$ is defined as:

$$\Delta^{25}\text{Mg}' = \delta^{25}\text{Mg}' - 0.521 \times \delta^{26}\text{Mg}' \quad (4)$$

and the linearized form of δ (δ') defined as:

$$\delta^x\text{Mg}' = \ln \left[\frac{\left(\frac{^x\text{Mg}}{^{24}\text{Mg}} \right)_{\text{sample}}}{\left(\frac{^x\text{Mg}}{^{24}\text{Mg}} \right)_{\text{DSM-3}}} \right] \times 10^3 \quad (5)$$

Where $x = 25$ or 26 . The use of the linearized form of the δ is, however, most useful in extremely fractionated systems given that the difference between $\delta^{25}\text{Mg}'$ and $\delta^{26}\text{Mg}$ is only 1 ppm per 2 of mass dependant fractionation, which is well within the analytical uncertainty quoted by most laboratories for the $\delta^{25}\text{Mg}$ value. In the case of our study, the $\Delta^{25}\text{Mg}'$ and $\mu^{26}\text{Mg}^*$ provide the same information regarding the analysis of the fractionation law, but the $\Delta^{25}\text{Mg}'$ parameter emphasizes deviation from the equilibrium law whereas the $\mu^{26}\text{Mg}^*$ value expresses deviations from the kinetic law. We report the $\mu^{26}\text{Mg}^*$ instead of the $\Delta^{25}\text{Mg}'$ value as it allows us to directly compare our data with other high-precision Mg-isotope studies of extraterrestrial materials where the $\mu^{26}\text{Mg}^*$ is more commonly reported.

Using our approach, typical uncertainties (2 se) for a single analysis (1667 s of data acquisition) are typically ~ 4 , 5 and 10 ppm for the $\mu^{26}\text{Mg}^*$, $\mu^{25}\text{Mg}$ and $\mu^{26}\text{Mg}$, respectively. Pooling the data over 10 analyses results in weighted means with typical uncertainties (2 se) of ~ 1.5 , 10 and 20 ppm for the $\mu^{26}\text{Mg}^*$, $\mu^{25}\text{Mg}$ and $\mu^{26}\text{Mg}$, respectively. We have calculated the theoretical limit for the uncertainty of the $\mu^{26}\text{Mg}^*$ value for a single measurement (*i.e.* 1667 s of data acquisition), considering the total number of ions collected, the baseline parameters, the level of Johnson-Nyquist resistor noise, and the Poisson noise arising from counting discrete particles. Given that data for this study was collected at signal intensities that exceed the threshold where the Johnson-Nyquist is no longer a source of noise in the measurement ($\sim 0.100\text{V}$; ref. 38), the main source of error on the precision of the $\mu^{26}\text{Mg}^*$ value originates from the Poisson noise and, thus, we calculate a theoretical limit of 3.5 ppm for the uncertainty of the $\mu^{26}\text{Mg}^*$. Given the typical internal error of ~ 4 ppm obtained on single measurements, this indicates that the majority of the

uncertainty in the $\mu^{26}\text{Mg}^*$ ($>85\%$) can be ascribed to counting statistics, and the remainder of the instrument parameters only contribute to a minor extent to the total uncertainty.

Absolute Mg-isotope analyses (403 s duration, $\sim 12\text{V}$ of ^{24}Mg) had uncertainties per analysis of 15–20 and 20–25 ppm for the $^{25}\text{Mg}/^{24}\text{Mg}$ and $^{26}\text{Mg}/^{24}\text{Mg}$ ratios, respectively. Bracketing consisted of 11 spiked analyses and 10 unspiked analyses, and typically resulted in weighted averages with a precision of 10 to 20 ppm for absolute $^{25}\text{Mg}/^{24}\text{Mg}$ ratios and 15 to 30 ppm for absolute $^{26}\text{Mg}/^{24}\text{Mg}$ ratios. Data were reduced using a mass discrimination exponent (β) of 0.500 (similar to the power law, which has a β of 0.501) to correct for instrumental mass discrimination.

3 Results and discussion

3.1 Sample introduction system

During the course of this study, we evaluated the performance of two introduction systems suitable for high-precision Mg-isotope ratio measurements, namely the ThermoFisher stable introduction system (SIS, wet plasma) and the Aridus II desolvating nebulizer (dry plasma). Our primary goal was to identify which of the two systems is most stable during an entire analytical session, which corresponds typically to 36 to 60 h of continuous measurement without adjusting the instrument's tuning parameters. However, initial testing with the Aridus II suggested that frequent adjustments of the sweep gas settings (Ar and N_2) were required to ensure that no significant drifts ($<20\%$) in signal intensity occurred over periods of $\sim 12\text{h}$. Therefore, the Aridus II introduction system was deemed unsuitable for our approach and, hence, all data in this study were acquired with the SIS, which provides greater stability in signal intensities over periods $>24\text{h}$. Using the SIS, typical drifts in the in the $\mu^{26}\text{Mg}^*$, $\mu^{25}\text{Mg}$ and total Mg ion intensity were ~ 40 ppm, ~ 1000 ppm and 25%, respectively, over a period of 48 h without adjusting the instrument's tuning parameters.

A marked disadvantage of the SIS is the reduced transmission as compared to that obtainable with the Aridus desolvating nebulizer. To compensate for this poorer sensitivity, we have combined the SIS with a skimmer cone characterized by a greater aperture (the so-called X-cone), which allowed us to routinely obtain a sensitivity of $\sim 20\text{V/ppm}$ for Mg in medium resolution mode. The use of the X-cone, however, dramatically reduces the lifespan of the entrance slit (or resolution slit). We noted a significant degradation of the instrument's resolving power after only $\sim 350\text{h}$ of continuous measurements due to the gradual physical deterioration of the entrance slit, which required periodical replacement of the tongue-slit assembly.

The use of high-sensitivity skimmer cones such as the X-cone can enhance oxide and, possibly, hydride production close to the skimmer surface.³⁹ As such, enhanced hydride production may affect the accuracy of the data presented in this study given that the potentially interfering $^{24}\text{MgH}^+$ species is only resolved at the $\sim 70\%$ level. We have investigated the potential effect of $^{24}\text{MgH}^+$ interference of the ^{25}Mg peak by comparing the internally normalized $^{26}\text{Mg}/^{24}\text{Mg}$ ratios obtained on standard solutions run at different Mg concentrations. However, no resolvable effects were observed when the concentration of the standard solutions

were within 20%. Nevertheless, sample and standard solutions measured in each analytical session were adjusted to have the same Mg concentration within 2%, so that any effect arising from potential plasma-based interferences was the same in each case.

3.2 Correction of instrumental mass discrimination

Instrumental mass discrimination is a major obstacle for the acquisition of precise and accurate isotope ratio data in plasma source mass spectrometry. The nature of the processes controlling mass discrimination and the choice of which law to use when correcting for mass discrimination is a matter of debate,^{40–45} and has the potential to significantly impact results. Although it is not possible to determine the exact nature of mass fractionation without using a reference standard of known absolute isotopic composition, some information can be derived from our data. First, we observe that drift in $^{25}\text{Mg}/^{24}\text{Mg}$ and $^{26}\text{Mg}/^{24}\text{Mg}$ ratios within a session always occurs along a fractionation curve that has an exponent (β) varying between sessions from 0.499 and 0.501 (*e.g.* Fig. 1). Although it is possible that this drift is related to only part of the total instrumental mass discrimination, it does confirm that at least one component of the mass discrimination is well modeled using the power law. Second, absolute Mg-isotope ratios obtained using the double-spike method vary up to 50% more between analytical sessions when corrected with an exponential law as compared to a β of 0.500. The superior reproducibility of the latter thus provides further evidence that mass discrimination is best modeled using a β of 0.500. Based on these premises, we correct mass discrimination in absolute Mg-isotope measurements using a β of 0.500 (*i.e.* a near-power law, which has a β of 0.501, *ref.* 46). Note, however, that when measuring relative Mg-isotope ratios to obtain $^{26}\text{Mg}^*$ we use an exponential equation to correct for mass discrimination to minimize the risk of introducing analytical artifacts to the data (see section 3.4). This is because our approach was essentially developed to search for $^{26}\text{Mg}^*$ anomalies in extraterrestrial materials with a naturally fractionated Mg-isotope composition that is best approximated by kinetic processes such as, for example, calcium-aluminium-rich inclusions.

A number of earlier studies^{46–48} have suggested that instrumental mass discrimination in MC-ICPMS is best explained by a process intermediate to kinetic and equilibrium mass fractionation, which is in apparent contradiction to our findings. However, these studies were based on heavier elements such as hafnium and neodymium and, in principle, it is possible that the mass discrimination of light elements like Mg is better described by a power law. A further important point is that we have used a skimmer cone (X-cone) with a modified geometry, which is well known to significantly impact instrumental mass discrimination.³⁹ Therefore, it is unlikely that these earlier results apply to our study, and we suggest that our attempt to model the instrumental mass discrimination by examining long term instrumental drift (>35 h, Fig. 1) within analytical sessions is a valid approach.

3.3 Reproducibility and accuracy of Mg-isotope measurements

The long-term reproducibility and accuracy of our Mg-isotope data was evaluated by (a) analyzing a number of terrestrial rock

samples (BHVO-2, BIR-1 and DTS-2), (b) duplicate analyses of terrestrial and meteorite samples, including analyzing 7 aliquots of the DTS-2 rock standard, 5 aliquots of olivine crystals separated from the J12 spinel lherzolite as well as 5 aliquots of a homogenized powder of the SAH 97159 enstatite chondrite, (c) doping an in-house Mg standard solution with a ^{26}Mg spike (99% pure) to create gravimetrically determined ^{26}Mg excesses, and (d) doping a Mg-free sample matrix with Mg of known composition and processing this mixture through our Mg purification protocol.

Analysis of the DTS-2, J-12 and SAH 97159 enstatite chondrite samples provides a means to evaluate the reproducibility of the $\mu^{25}\text{Mg}$ value, given that these represent initially homogenized solutions divided into different aliquots and individually processed through our Mg purification protocol. As illustrated in Table 2 the various aliquots of these three samples, typically analyzed in different analytical sessions during the course of this study, all reproduced to better than 20 ppm for the $\mu^{25}\text{Mg}$ value. Thus, we conclude that an accuracy and reproducibility of 20 ppm can be routinely obtained for the $\mu^{25}\text{Mg}$ value using the analytical protocols presented in this study. Moreover, we have also analyzed a Mg-free sample matrix (refractory inclusion from the Efremovka chondrite) doped with Mg of known isotopic composition (that is, an in-house Mg standard solution) that was processed through our chemical separation protocol. As shown in Table 1, the $\mu^{25}\text{Mg}$ value obtained for the rock matrix is identical to that of the unprocessed Mg standard solution within the estimated reproducibility of 20 ppm, suggesting that our Mg purification protocol does not introduce undesirable analytical artifacts.

The seven and five aliquots of the DTS-2 and J12 olivine samples yield $\mu^{26}\text{Mg}^*$ values of 0.9 ± 1.7 and -0.4 ± 1.7 ppm, respectively (Table 2). Pooling these analyses with all terrestrial rock samples analyzed in this study yield a $\mu^{26}\text{Mg}^*$ value of 0.3 ± 2.3 ppm. The five aliquots of the SAH 97159 enstatite chondrite define a $\mu^{26}\text{Mg}^*$ value of 0.3 ± 1.8 ppm (Table 2). The sample matrix doped with natural Mg returned a $\mu^{26}\text{Mg}^*$ value of -0.5 ± 2.5 ppm (Table 2), indicating that the Mg purification technique does not affect the integrity of the $\mu^{26}\text{Mg}^*$ data. We have also gravimetrically doped an in-house Mg standard with pure ^{26}Mg spike to create an excess of 5 ppm in the $\mu^{26}\text{Mg}^*$ value. Five replicate analyses of this solution analyzed during different analytical sessions throughout this study yielded a $\mu^{26}\text{Mg}^*$ value of 4.8 ± 2.5 ppm (Table 3). Based on these experiments, we estimate the accuracy and reproducibility of our approach to be 2.5 ppm for the $\mu^{26}\text{Mg}^*$ value.

The analytical reproducibility of the ^{24}Mg - ^{26}Mg double-spike method for absolute Mg-isotope ratios was evaluated using duplicate analyses of several commonly used reference and in-house standards (DSM-3, Cambridge-1 and J12 olivine). Between these duplicate analyses the machine was turned off, the cones were cleaned and gains were calibrated to ensure that any causes of bias were accounted for. Based on these results (Table 4), we estimate the external reproducibility of our analyses to be 35 and 36 ppm for absolute $^{25}\text{Mg}/^{24}\text{Mg}$ and $^{26}\text{Mg}/^{24}\text{Mg}$ ratios, respectively. However, as noted in Section 2.5, although these values are the limit to which we can resolve differences between the absolute isotope ratios of samples, systematic errors in the composition of the double-spike limit the accuracy of the absolute ratios to 195 ppm for $^{25}\text{Mg}/^{24}\text{Mg}$ ratios and 235 ppm for $^{26}\text{Mg}/^{24}\text{Mg}$ ratios.

Table 2 Mg-isotope composition of terrestrial and extraterrestrial reservoirs relative to DSM-3

Sample	type of material	$\mu^{26}\text{Mg}^*$	$\mu^{25}\text{Mg}$	$\mu^{26}\text{Mg}$	<i>N</i>
DTS-2 (1)	dunite	-0.8 ± 2.2	-115 ± 7	-221 ± 19	10
DTS-2 (2)	dunite	1.6 ± 1.6	-119 ± 8	-224 ± 21	10
DTS-2 (3)	dunite	1.3 ± 1.8	-113 ± 11	-212 ± 25	10
DTS-2 (4)	dunite	0.4 ± 1.2	-137 ± 10	-261 ± 23	10
DTS-2 (5)	dunite	1.6 ± 1.6	-122 ± 8	-231 ± 20	10
DTS-2 (6)	dunite	1.0 ± 1.2	-124 ± 15	-236 ± 33	10
DTS-2 (7)	dunite	1.3 ± 1.5	-121 ± 17	-227 ± 35	10
<i>Average and 2sd</i>		0.9 ± 1.7	-122 ± 17	-230 ± 31	7
J12 (1)	mantle olivine	0.9 ± 1.8	-156 ± 4	-308 ± 9	10
J12 (2)	mantle olivine	-0.7 ± 1.4	-158 ± 10	-290 ± 21	10
J12 (3)	mantle olivine	0.1 ± 1.4	-153 ± 6	-299 ± 13	10
J12 (4)	mantle olivine	-1.0 ± 1.6	-145 ± 10	-283 ± 16	10
J12 (5)	mantle olivine	-1.3 ± 0.7	-154 ± 10	-301 ± 19	10
<i>Average and 2sd</i>		-0.4 ± 1.7	-153 ± 11	-296 ± 19	5
BHVO-2	basalt	-0.4 ± 1.2	-101 ± 9	-189 ± 23	10
BIR-2	basalt	-1.6 ± 1.8	-111 ± 9	-210 ± 23	10
OSIL	north Atlantic seawater	11.6 ± 1.6	-482 ± 10	-933 ± 20	10
IPASO (batch p151)	mid Atlantic seawater	13.3 ± 2.1	-511 ± 9	-986 ± 17	10
SAH 97159 (1)	enstatite chondrite	0.7 ± 1.6	-127 ± 13	-245 ± 27	10
SAH 97159 (2)	enstatite chondrite	-0.3 ± 1.2	-121 ± 12	-230 ± 28	10
SAH 97159 (3)	enstatite chondrite	-0.7 ± 2.1	-136 ± 11	-259 ± 26	10
SAH 97159 (4)	enstatite chondrite	0.3 ± 1.9	-125 ± 16	-238 ± 36	10
SAH 97159 (5)	enstatite chondrite	1.7 ± 1.2	-142 ± 9	-277 ± 19	10
<i>Average and 2sd</i>		0.3 ± 1.8	-130 ± 17	-250 ± 37	5
NWA 856	martian shergottite	-2.3 ± 1.8	-134 ± 6	-258 ± 18	10
Refractory inclusion ^a	Mg standard + sample matrix	-0.5 ± 2.5	-10 ± 8	-29 ± 23	10

The DTS-2, J12 and SAH 97159 replicate analyses represent single sample digestions divided into a number of aliquots that were individually processed through our Mg purification protocol.^a We doped the Mg-free matrix of an amoeboid olivine aggregate from the Efremovka chondrite (AOA; sample ES3 from Larsen *et al.*⁵³) with an in-house Mg standard and processed this mixture through our separation protocol.

3.4 Mass-dependent Mg-isotope fractionation and the $\mu^{26}\text{Mg}^*$ value

A potential limitation to high-precision determination of the $\mu^{26}\text{Mg}^*$ value is the degree and nature of the mass-dependent isotope fractionation affecting the material analyzed. Because it is not possible to distinguish between the instrumental and natural mass fractionation during analysis of unknown samples by MC-ICPMS, a central assumption in our approach is that both instrumental and natural mass fractionation follow the same fractionation law. Analysis of material with a Mg-isotope

composition naturally fractionated following a process that is different to that driving the instrumental mass fractionation may lead to apparent excesses or deficits in the $\mu^{26}\text{Mg}^*$ value. In Fig. 2, we illustrate this effect for a hypothetical material that has experienced variable mass-dependent equilibrium fractionation as compared to the reference standard, and analyzed on an MC-ICPMS where the instrumental mass discrimination is solely driven by a kinetic process (*i.e.* modeled by the exponential law). We note that the apparent excess/deficit in the $\mu^{26}\text{Mg}^*$ resulting from inappropriate mass discrimination correction is ~ 4 ppm per 100 ppm of mass-dependent fractionation as recorded by the

Table 3 Relative Mg-isotope composition of synthetic standard solutions

Sample	$\mu^{26}\text{Mg}^*$	$\mu^{25}\text{Mg}$	$\mu^{26}\text{Mg}$	<i>N</i>
Aristar + 5ppm (1)	4.5 ± 1.6	0 ± 5	14 ± 13	10
Aristar + 5ppm (2)	4.0 ± 1.5	-8 ± 9	-9 ± 17	10
Aristar + 5ppm (3)	7.0 ± 1.4	3 ± 11	13 ± 22	10
Aristar + 5ppm (4)	4.6 ± 1.3	11 ± 10	26 ± 19	10
Aristar + 5ppm (5)	3.9 ± 1.6	-10 ± 8	-16 ± 14	10
<i>Average and 2sd</i>	4.8 ± 2.5	-1 ± 17	6 ± 35	5
Aristar _{DSM-3}	21.6 ± 1.6	-811 ± 7	-1566 ± 13	10
Alfa Aesar-1 _{DSM-3}	22.0 ± 2.3	-534 ± 8	-1022 ± 14	10
Alfa Aesar-2 _{DSM-3}	21.8 ± 2.5	-1728 ± 8	-3357 ± 15	10
Cambridge-1 _{DSM-3}	25.1 ± 2.1	-1326 ± 12	-2568 ± 25	10

An aliquot of the Aristar standard was doped with a ^{26}Mg spike to create a gravimetrically determined 5 ppm $\mu^{26}\text{Mg}^*$ excess and analyzed against the pure Aristar standard 5 times during distinct analytical sessions. All other synthetic standards were analyzed against DSM-3.

Table 4 Absolute Mg-isotope composition of synthetic standard solutions and chondrites

Sample	Type of material	$^{25}\text{Mg}/^{24}\text{Mg}$ ($\pm 2\text{se}$)	$^{26}\text{Mg}/^{24}\text{Mg}$ ($\pm 2\text{se}$)	N
DSM-3 (1)	Synthetic standard	0.1269139 (13)	0.1396939 (31)	9
DSM-3 (2)	Synthetic standard	0.1269124 (20)	0.1396883 (42)	10
DSM-3 (3)	Synthetic standard	0.1269137 (18)	0.1396905 (29)	10
DSM-3 (4)	Synthetic standard	0.1269134 (13)	0.1396880 (23)	10
DSM-3 (5)	Synthetic standard	0.1269147 (09)	0.1396953 (15)	10
DSM-3 (6)	Synthetic standard	0.1269167 (18)	0.1396873 (34)	10
<i>Average and 2sd</i>		<i>0.1269141</i> (29)	<i>0.1396906</i> (67)	6
Cambridge-1 (1)	Synthetic standard	0.1267402 (15)	0.1393242 (24)	10
Cambridge-1 (2)	Synthetic standard	0.1267414 (06)	0.1393244 (23)	3
Cambridge-1 (3)	Synthetic standard	0.1267431 (12)	0.1393228 (17)	6
Cambridge-1 (4)	Synthetic standard	0.1267455 (25)	0.1393256 (50)	9
Cambridge-1 (5)	Synthetic standard	0.1267434 (18)	0.1393278 (39)	9
Cambridge-1 (6)	Synthetic standard	0.1267493 (25)	0.1393243 (32)	8
<i>Average and 2sd</i>		<i>0.1267438</i> (65)	<i>0.1393249</i> (34)	6
<i>Deviation from DSM-3 (in ppm)</i>		<i>−1342</i>	<i>−2618</i>	
J12 (1)	mantle olivine	0.1268935 (23)	0.1396483 (41)	10
J12 (2)	mantle olivine	0.1268950 (17)	0.1396502 (40)	10
J12 (3)	mantle olivine	0.1268978 (27)	0.1396529 (39)	10
J12 (4)	mantle olivine	0.1268966 (11)	0.1396547 (29)	10
<i>Average and 2sd</i>		<i>0.1268957</i> (38)	<i>0.1396515</i> (57)	4
<i>Deviation from DSM-3 (in ppm)</i>		<i>−145</i>	<i>−279</i>	
Orgueil	CI chondrite	0.1269002 (18)	0.1396477 (30)	10
<i>Deviation from DSM-3 (in ppm)</i>		<i>−110</i>	<i>−307</i>	
Alais	CI chondrite	0.1268966 (12)	0.1396423 (23)	10
<i>Deviation from DSM-3 (in ppm)</i>		<i>−138</i>	<i>−345</i>	

Deviation from DSM-3 is quoted relative to the average values provided here, with estimated uncertainties of 35 and 36 ppm for $^{25}\text{Mg}/^{24}\text{Mg}$ and $^{26}\text{Mg}/^{24}\text{Mg}$ ratios, respectively.

$\mu^{25}\text{Mg}$ value. This highlights the potential pitfalls in attempting to accurately identify small $\mu^{26}\text{Mg}^*$ excesses or deficits in extra-terrestrial materials characterized by a fractionated Mg-isotope composition as compared to that of the reference standard.

We have further investigated these effects by analyzing a number of commercially available synthetic Mg standard solutions as well as the Cambridge-1 Mg standard, using DSM-3 as our reference standard. All materials analyzed are typified by a light Mg-isotope composition as compared to DSM-3 ($\mu^{25}\text{Mg}$ ranging from ~ -500 to -1700 ppm), and with clearly resolved excesses in $\mu^{26}\text{Mg}^*$ varying from ~ 20 to 25 ppm (Table 3). These apparent excesses in $\mu^{26}\text{Mg}^*$ reflect variable components of mass-dependent equilibrium fractionation affecting the natural fractionation processes of these materials. For example, the Mg-isotope composition of the Alfa Aesar-1 synthetic solution can be explained by pure thermodynamic equilibrium fractionation, whereas the Alfa Aesar-2 synthetic solution reflects only $\sim 34\%$ of equilibrium fractionation, assuming that the original composition of these materials was similar to DSM-3. The $\mu^{25}\text{Mg}$ value of -1326 ± 12 ppm obtained here for the Cambridge-1 standard compares favorably with previous studies,^{10,24,49} although these have analytical uncertainties that typically 5 to 10 times larger.

As demonstrated by a number of previous studies,^{8–18} the DSM-3 Mg standard is isotopically heavier than Earth's mantle by ~ 150 ppm for the $\mu^{25}\text{Mg}$ value. This standard has been generated by the industrial purification of brine and, therefore, may have been fractionated during the purification process. This raises the possibility that, similarly to the synthetic Mg standards discussed above, the DSM-3 standard carries a component of

equilibrium mass dependent fractionation. This would result in systematically introducing biases of up to +6 ppm in the $\mu^{26}\text{Mg}^*$ of mantle-derived samples when measured against DSM-3. However, our replicate measurements of terrestrial mantle-derived rocks analyzed against the DSM-3 standard define a $\mu^{26}\text{Mg}^*$ value of 0.9 ± 1.7 , indicating that no significant component of equilibrium mass dependent fractionation is present in DSM-3. Therefore, this reference material is appropriate for the identification of small $\mu^{26}\text{Mg}^*$ anomalies in extra-terrestrial materials.

3.5 The relative Mg-isotope composition of various terrestrial and extraterrestrial reservoirs

We show in Fig. 3 the $\mu^{25}\text{Mg}$ values for mantle-derived terrestrial samples, the Martian shergottite NWA 856 and the enstatite chondrite SAH 97159. All inner solar system silicate materials analyzed show a restricted range of $\mu^{25}\text{Mg}$ values ranging from -153 ± 11 to -101 ± 9 ppm. No systematic difference is observed between terrestrial and extraterrestrial materials, with the martian and enstatite chondrite meteorites having $\mu^{25}\text{Mg}$ values within the range of our terrestrial samples. We note that the range of $\mu^{25}\text{Mg}$ present in mantle-derived samples is marginally out of analytical uncertainty by ~ 10 ppm, considering the external reproducibility of 20 ppm for $\mu^{25}\text{Mg}$ using our approach. However, the material defining the lowest $\mu^{25}\text{Mg}$ analyzed in this study are olivine crystals separated from the J12 mantle xenolith. This may reflect a minor component of Mg-isotope fractionation amongst co-existing mantle minerals, as suggested by previous studies.^{11,50} When

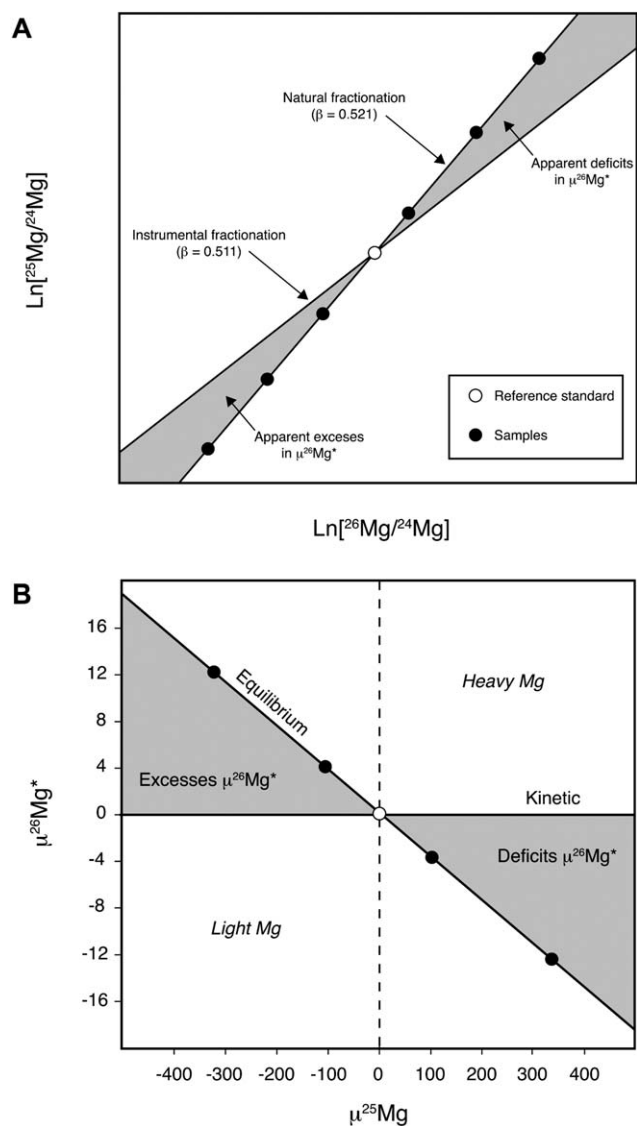


Fig. 2 Magnesium three isotope diagrams for hypothetical samples having experienced mass-dependent equilibrium ($\beta = 0.521$) fractionation and analyzed on a mass spectrometer where the instrumental fractionation is dominated by a kinetic process ($\beta = 0.511$). (A) Plotted are the natural logarithms of the raw $^{25}\text{Mg}/^{24}\text{Mg}$ and $^{26}\text{Mg}/^{24}\text{Mg}$ ratios. (B) Plotted as the $\mu^{26}\text{Mg}^*$ value as a function of the $\mu^{25}\text{Mg}$ value. Areas in gray define regions typified by apparent excesses or deficits in both diagrams. The apparent excess/deficit in the $\mu^{26}\text{Mg}^*$ resulting from inappropriate mass discrimination correction is ~ 4 ppm per 100 ppm of mass-dependent fractionation as recorded by the $\mu^{25}\text{Mg}$ value.

considering bulk material only, all samples analyzed in this study are identical within analytical uncertainty, defining a $\mu^{25}\text{Mg}$ value of -120 ± 28 ppm (2sd) relative to DSM-3. Moreover, the martian and enstatite chondrite meteorites returned $\mu^{26}\text{Mg}^*$ values identical to the bulk silicate Earth, taking into account the external reproducibility of 2.5 ppm for this value. These results suggest that Mg-isotope fractionation by high temperature processes does not play an important role during planetary differentiation, and, therefore, that the bulk Mg-isotope composition of the inner solar system is uniform within the resolution of our analyses.

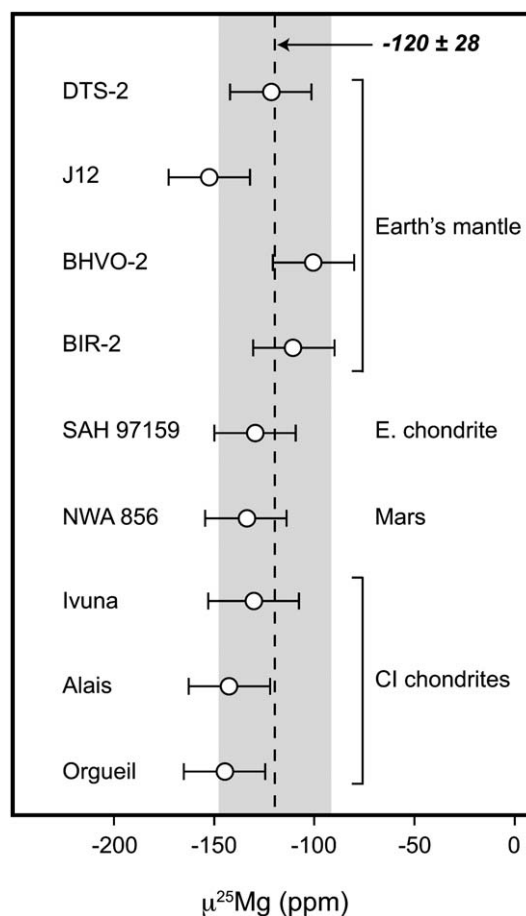


Fig. 3 High-precision Mg-isotope composition of inner solar system materials relative to DSM-3. The CI chondrites data are from Larsen *et al.*,⁵³ and were obtained using the same analytical protocols used in this study. The dotted line and gray band represent the average and 2sd of the bulk samples analysed in this study (DTS-2, BHVO-2, BIR-2, SAH 97159, NWA 856). Analytical uncertainty represents the internal error or external reproducibility (20 ppm), whichever is larger. E., enstatite.

We have also analyzed two seawater samples provided by OSIL, derived from the mid and north Atlantic ocean (Table 2). The north Atlantic sample yielded a $\mu^{25}\text{Mg}$ value of -482 ± 10 ppm whereas the mid atlantic sample returned a $\mu^{25}\text{Mg}$ of -511 ± 9 ppm. Given the estimated external reproducibility of 20 ppm for the $\mu^{25}\text{Mg}$ value using our approach, these results are consistent with the theory that the Mg-isotope composition of seawater is constant, in agreement with previous studies.³⁷ However, we note that the $\mu^{25}\text{Mg}$ values reported here for seawater are marginally lighter (50–75 ppm) than that obtained in a number of previous studies.^{9,10,37,51} Given the improved Mg purification scheme employed in our study, we speculate that the data presented in previous studies may be compromised by the presence of residual matrix, which typically tends to induce apparent heavier compositions.

Both seawater samples returned clearly resolved excesses in $\mu^{26}\text{Mg}^*$ of 13.0 ± 2.1 ppm and 10.1 ± 3.6 ppm for the mid and north Atlantic samples, respectively. This result indicates that a significant component of equilibrium mass dependent fractionation is associated with the flux and/or sink of Mg to the

modern oceans as compared to the Mg composition of the bulk silicate Earth. We highlight that the improved resolution of our approach in determining the $\mu^{26}\text{Mg}^*$ and, hence in assessing the nature of the fractionation processes, may allow for a better understanding of the global Mg cycle in future studies.

Based on a limited dataset, Wiechert and Halliday⁵² argued that there are detectable differences in the Mg-isotope composition of upper mantle peridotites and bulk chondrites. Based on this result, these authors proposed that the Earth was formed by preferential sorting of chondrules characterized by a heavier Mg-isotope composition. Following this proposal, a number of studies^{8–18,53} have demonstrated, based on much larger datasets, that the Mg-isotope composition of Earth's mantle is identical to chondrite meteorites within a typical resolution of $\sim 50\text{--}75$ ppm for the $\mu^{25}\text{Mg}$ value, defining a $\mu^{25}\text{Mg}$ value relative to the DSM-3 standard of ~ -125 ppm. Our result are consistent with these studies, although the external reproducibility of our $\mu^{25}\text{Mg}$ data using the approach presented here is 2 to 3 times better than previously achievable.

Similarly to Wiechert and Halliday,⁵² it has been recently suggested that carbonaceous chondrites are systematically lighter by ~ 50 ppm in their $\mu^{25}\text{Mg}$ values than Earth's mantle.⁵⁰ However, we note that Larsen *et al.*⁵³ recently reported high-precision Mg-isotope measurements for three CI carbonaceous chondrites, namely Orgueil, Alais and Ivuna. These yield an average $\mu^{25}\text{Mg}$ value of -136 ± 30 ppm, which is identical to the terrestrial and extraterrestrial samples studied here. Given that none of the recent studies based on more extensive datasets have observed any discrepancy, the systematic difference between carbonaceous chondrites and Earth's mantle observed by Young *et al.*⁵⁰ may reflect a sampling bias or, alternatively, an analytical artifact.

Chakrabarti and Jacobsen⁵¹ recently proposed a different Mg-isotope composition for inner solar system silicate rocks, based on a suite of primitive and differentiated meteorites as well as terrestrial rocks. They suggested a homogenous inner solar system composition with a $\mu^{25}\text{Mg}$ value of -273 ± 28 ppm relative to the DSM-3 standard. This composition is approximately 100 ppm lighter than previously reported by most recent high-precision Mg-isotope studies, including the results presented in the current work. Although the reason for the systematic offset in the data of Chakrabarti and Jacobsen⁵¹ remains unclear, the concordancy between the absolute and relative composition of inner solar materials relative to the DSM-3 standard obtained in our study does not support the result of Chakrabarti and Jacobsen.⁵¹

3.6 The absolute Mg-isotope composition of bulk silicate Earth, CI chondrites and reference standards

We have determined the absolute Mg-isotope composition of the DSM-3 and Cambridge-1 terrestrial standards, olivine crystals separated from a spinel lherzolite (J12 olivines), as well as the Orgueil and Alais CI chondrites (Table 4). Based on these results, we calculate a difference between the absolute $^{25}\text{Mg}/^{24}\text{Mg}$ ratios of the J12 olivines, the Orgueil and Alais CI chondrites and the Cambridge-1 standard relative to the DSM-3 standard of -145 ± 50 ppm, -110 ± 50 ppm, -138 ± 50 ppm, and -1342 ± 62 ppm, respectively. These results are in excellent agreement with

those obtained by the sample-standard bracketing method presented in section 3.5. Based on the averages obtained for the J12 olivine separates, we estimate the absolute Mg-isotope composition for Earth's mantle to be $^{25}\text{Mg}/^{24}\text{Mg} = 0.126896 \pm 0.000025$ and $^{26}\text{Mg}/^{24}\text{Mg} = 0.139652 \pm 0.000033$ (quoted uncertainties are 95% confidence intervals, taking into account all known sources of uncertainty). However, we emphasize that the accuracy of the absolute $^{25}\text{Mg}/^{24}\text{Mg}$ reported here is dependent on the validity of our assumption that the instrumental drift within analytical sessions (Fig. 1), which is best modeled by a mass fractionation law with a $\beta = 0.500$, is representative of the instrumental mass bias of our instrument under the analytical conditions employed for Mg-isotope measurements. Given that we used a $^{26}\text{Mg}\text{-}^{24}\text{Mg}$ spike, this concern does not apply to the accuracy of the absolute $^{26}\text{Mg}/^{24}\text{Mg}$ ratio. If our assumption is not valid and the instrument mass discrimination is, in fact, best explained by a kinetic process ($\beta = 0.511$), then our proposed $^{25}\text{Mg}/^{24}\text{Mg}$ value may be inaccurate by ~ 1100 ppm, although the $^{26}\text{Mg}/^{24}\text{Mg}$ will remain unchanged.

Recent work suggests that Mg-isotope fractionation may arise between mineral phases during crystallization,^{11,50} which would potentially compromise the relevance of using J12 to estimate the composition of Earth's mantle. However, our higher precision measurements obtained by the sample-standard bracketing method (Section 3.5) of both the J12 olivine separate and the DTS-2 dunite obtained by sample-standard bracketing indicate that although subtle differences ($\mu^{25}\text{Mg}$ of ppm ~ 30 and $\mu^{26}\text{Mg}$ of ~ 60 ppm) may exist between these materials, they are indistinguishable at the resolution of the double-spike method, and significantly less than the total uncertainties on the ratios. As such, until further improvements are made to the measurement of absolute Mg-isotopic compositions J12 olivine is a suitable proxy for Earth's mantle.

Given the restricted range in $^{25}\text{Mg}/^{24}\text{Mg}$ compositions for bulk inner solar system planetary materials determined here by the sample-standard bracketing method, and the excellent agreement with the absolute method, we propose that the new values of $^{25}\text{Mg}/^{24}\text{Mg} = 0.126896$ and $^{26}\text{Mg}/^{24}\text{Mg} = 0.139652$ suggested here for the absolute Mg-isotope composition of Earth's mantle represents that of the bulk inner solar system.

These values are not within uncertainties of the ratios of $^{25}\text{Mg}/^{24}\text{Mg} = 0.12663 \pm 0.00013$ and $^{26}\text{Mg}/^{24}\text{Mg} = 0.13932 \pm 0.00026$ obtained by Catanzaro *et al.*,³⁴ but it should be noted that the SRM 980 reference standard characterized in that study was later shown to be heterogeneous to a significant degree.²⁴ If this heterogeneity is taken into account (approximately 1.7‰ and 3.2‰ on the $^{25}\text{Mg}/^{24}\text{Mg}$ and $^{26}\text{Mg}/^{24}\text{Mg}$ ratios, respectively), then the values obtained here are within the uncertainties of the previous study.

Using the absolute Mg-isotope composition of the J12 olivine obtained here and propagating estimated uncertainties using a Monte Carlo approach we have re-evaluated the isotopic abundances of Mg as $^{24}\text{Mg} = 0.789548 \pm 0.000026$, $^{25}\text{Mg} = 0.100190 \pm 0.000018$, and $^{26}\text{Mg} = 0.110261 \pm 0.000023$. Further, using the isotopic weights of Mg recommended by Audi *et al.*,⁵⁴ we have calculated an atomic weight (for $^{12}\text{C} = 12$) for Mg of 24.305565 ± 0.000045 u (unified atomic mass unit), this value is marginally heavier than the range previously determined by Catanzaro *et al.*,³⁰ and a factor of 10 more precise.

4 Conclusions

The main conclusions of this study can be summarized as follows:

1. Using improved techniques for the chemical purification and high-precision isotope measurements of Mg by HR-MC-ICPMS, it is possible to routinely measure the relative Mg-isotope composition of silicate materials with an external reproducibility of 2.5 and 20 ppm for the $\mu^{26}\text{Mg}^*$ and $\mu^{25}\text{Mg}$ values, respectively.

2. High-precision analyses of bulk mantle-derived rocks as well as a martian shergottite and enstatite chondrite define the restricted range of $\mu^{25}\text{Mg}$ of -120 ± 28 ppm (2 sd) relative to DSM-3, suggesting that the Mg-isotope composition of inner solar system bulk planetary materials is uniform within the resolution of our analyses. These results are consistent with most recent studies,^{8–18} although the resolution of our analyses is a factor of 5 to 10 better. Repeated analyses of olivine crystals separated from a mantle-derived spinel lherzolite return the $\mu^{25}\text{Mg}$ value of -153 ± 11 ppm (2sd), which is marginally lighter than the bulk rocks analyzed in our study. This may reflect a minor component of Mg-isotope fractionation amongst coexisting mantle mineral, as suggested by previous studies.^{11,50}

3. The improved resolution of the $\mu^{26}\text{Mg}^*$ allows for a better assessment of the nature of the fractionation processes affecting terrestrial and extraterrestrial materials. The resolved excesses in $\mu^{26}\text{Mg}^*$ of ~ 10 ppm for two Atlantic seawater samples suggests that a significant component of equilibrium mass dependent fractionation is associated with the flux and/or sink of Mg to the modern oceans as compared to the Mg composition of the bulk silicate Earth. Replicate measurements of terrestrial mantle-derived rocks analyzed against the DSM-3 standard indicate that no significant component of equilibrium mass dependent fractionation is present in DSM-3. Therefore, this reference material is appropriate for the identification of small $\mu^{26}\text{Mg}^*$ anomalies in extraterrestrial materials.

4. Based on the averages obtained for the J12 olivine separates, we estimate the absolute Mg-isotope composition for Earth's mantle – and hence that of the bulk silicate Earth – to be $^{25}\text{Mg}/^{24}\text{Mg} = 0.126896 \pm 0.000025$ and $^{26}\text{Mg}/^{24}\text{Mg} = 0.139652 \pm 0.000033$. Given the restricted range of $\mu^{25}\text{Mg}$ obtained for bulk planetary material by the sample-standard bracketing technique and the excellent agreement between the data obtained by the relative and absolute methods, we propose that these new values represent the absolute Mg-isotope composition of the bulk inner solar system.

5. Using the absolute Mg-isotope composition of the J12 olivine, we calculate the isotopic abundances of Mg as $^{24}\text{Mg} = 0.789548 \pm 0.000026$, $^{25}\text{Mg} = 0.100190 \pm 0.000018$, and $^{26}\text{Mg} = 0.110261 \pm 0.000023$. Based on this result, we have calculated an atomic weight for Mg of 24.305565 ± 0.000045 .

6. The results we present for the relative Mg-isotope composition of inner solar system materials are not consistent with the studies of Wiechert and Halliday⁵² and Young *et al.*,⁵⁰ which propose a non-chondritic Mg-isotope composition for the bulk silicate Earth. Similarly, the consistency between our results obtained by both the relative and absolute methods, which suggests a $\mu^{25}\text{Mg}$ value of ~ 120 ppm relative to DSM-3 for Earth's mantle, do not support the proposal of Chakrabarti and

Jacobsen⁵¹ that the Mg-isotope composition of the bulk silicate Earth is typified by a $\mu^{25}\text{Mg}$ value of -273 ± 28 ppm relative to the DSM-3 standard.

5 Acknowledgments

Financial support for this project was provided by the Danish National Research Foundation, the Danish Natural Science Research Council, and the University of Copenhagen's Programme of Excellence. The Centre for Star and Planet Formation is funded by the Danish National Research Foundation and the University of Copenhagen's Programme of Excellence. We thank the two anonymous referees for thorough and constructive comments, which greatly improve the quality of this paper.

6 References

- O. K. Manuel and G. Hwaung, *Meteoritics*, 1983, **18**, 209–222.
- C. M. Gray and W. Compston, *Nature*, 1974, **251**, 495–497.
- T. Lee, D. A. Papanastassiou and G. J. Wasserburg, *Geophys. Res. Lett.*, 1976, **3**, 109–112.
- S. S. Russell, G. Srinivasan, G. R. Huss and G. J. Wasserburg, *Science*, 1996, **273**, 757–762.
- T. Lee and D. A. Papanastassiou, *Geophys. Res. Lett.*, 1974, **1**, 225–228.
- G. J. Wasserburg, T. Lee and D. A. Papanastassiou, *Geophys. Res. Lett.*, 1974, **4**, 299–302.
- A. Galy, N. S. Belshaw, L. Halicz and R. K. O'Nions, *Int. J. Mass Spectrom.*, 2001, **208**, 89–98.
- F.-Z. Teng, M. Wadhwa and R. T. Helz, *Earth Planet. Sci. Lett.*, 2007, **261**, 8492.
- E. T. Tipper, P. Louvat, F. Capmas, A. Galy and J. Gaillardet, *Chem. Geol.*, 2008, **257**, 65–75.
- F. Wombacher, A. Eisenhauer, A. Heuserac and S. Weyer, *J. Anal. At. Spectrom.*, 2009, **24**, 627–636.
- M. Handler, J. A. Baker, M. Schiller, V. C. Bennett and G. M. Yaxley, *Earth Planet. Sci. Lett.*, 2009, **282**, 306–313.
- F.-Z. Teng, W. Y. Li, S. Ke, B. Marty, N. Dauphas, S. C. Huang, F. Y. Wu and A. Pourmand, *Geochim. Cosmochim. Acta*, 2010, **74**, 4150–4166.
- B. Bourdon, E. T. Tipper, C. Fitoussi and A. Stracke, *Geochim. Cosmochim. Acta*, 2010, **74**, 5069–5083.
- A. Galy, E. D. Young, R. D. Ash and R. K. O'Nions, *Science*, 2000, **290**, 1751–1753.
- M. Bizzarro, J. A. Baker and H. Haack, *Nature*, 2004, **431**, 275–278.
- J. Baker, M. Bizzarro, N. Wittig, J. Connelly and H. Haack, *Nature*, 2005, **436**, 1127–1131.
- M. Bizzarro, J. A. Baker, H. Haack and K. L. Lundgaard, *Astrophys. J.*, 2005, **632**, L41–L44.
- K. Thrane, M. Bizzarro and J. A. Baker, *Astrophys. J.*, 2006, **646**, L159–L162.
- B. Jacobsen, Q.-z. Yin, F. Moynier, Y. Amelin, A. N. Krot, K. Nagashima, I. D. Hutcheon and H. Palme, *Earth Planet. Sci. Lett.*, 2008, **272**, 353–364.
- Y. Amelin, A. N. Krot, I. D. Hutcheon and A. A. Ulyanov, *Science*, 2002, **297**, 1678–1683.
- J. N. Connelly, Y. Amelin, A. N. Krot and M. Bizzarro, *Astrophys. J.*, 2008, **675**, L121–L124.
- G. A. Brennecka, S. Weyer, M. Wadhwa, P. E. Janney, J. Zipfel and A. D. Anbar, *Science*, 2010, **327**, 449–451.
- J. E. Shaw, J. A. Baker, A. J. R. Kent, K. M. Ibrahim and M. A. Menzies, *J. Petrol.*, 2007, **48**, 1495–1512.
- A. Galy, O. Yoffe, P. E. Janney, R. W. Williams, C. Cloquet, O. Alard, L. Halicz, M. Wadhwa, I. D. Hutcheon, E. Ramon and J. Carignan, *J. Anal. At. Spectrom.*, 2003, **18**, 1352–1356.
- F. W. E. Strelow, *Anal. Chem.*, 1960, **32**, 1185–1188.
- F. W. E. Strelow, *Anal. Chim. Acta*, 1981, **127**, 63–70.
- F. W. E. Strelow, *Anal. Chem.*, 1984, **56**, 1053–1056.
- F. W. E. Strelow, A. H. Victor, C. R. van Zyl and Cynthia Eloff, *Anal. Chem.*, 1971, **43**, 870–876.

- 29 M. Schiller, J. Baker and M. Bizzarro, *Geochim. Cosmochim. Acta*, 2010, **74**, 4844–4864.
- 30 J. N. Connelly, D. G. Ulfbeck, K. Thrane, M. Bizzarro and T. Housh, *Chem. Geol.*, 2006, **233**, 126–136.
- 31 F. Albarède and B. L. Beard, in *Geochemistry of non-traditional stable isotopes*, ed. C. M. Johnson, B. L. Beard and F. Albarède, *Min. Soc. Am. and Geochem. Soc.*, Washington, 2004, pp. 113–152.
- 32 M. H. Dodson, *J. Sci. Instrum.*, 1963, **40**, 289–295.
- 33 J. G. S. Galer, *Chem. Geol.*, 1999, **157**, 255–274.
- 34 E. J. Catanzaro, T. J. Murphy, E. L. Garner and W. R. Shields, *Res. Nat. Bur. Stand.*, 1966, **70A**, 453–458.
- 35 V. Fournier, P. Marcus and I. Olefjord, *Surf. Interface Anal.*, 2002, **34**, 494–497.
- 36 C. Hellstrom, C. Paton, J. Woodhead and J. Hergt, *Mineralogical Association of Canada short course series*, 2008, **40**, 343–348.
- 37 E. D. Young and A. Galy, *Rev. Mineral. Geochem.*, 2004, **55**, 197–230.
- 38 D. Wielandt and M. Bizzarro, *J. Anal. At. Spectrom.*, 2011, **26**, DOI: 10.1039/c0ja00067a.
- 39 K. Newman, P. A. Freedman, J. Williams, N. S. Belshaw and A. N. Halliday, *J. Anal. At. Spectrom.*, 2009, **24**, 742–751.
- 40 G. R. Gillson, D. J. Douglas, J. E. Fulford, K. W. Halligan and S. D. Tanner, *Anal. Chem.*, 1988, **60**, 1472–1474.
- 41 L. A. Allen, J. J. Leach and R. S. Houk, *Anal. Chem.*, 1997, **69**, 2384–2391.
- 42 D. J. Douglas and S. D. Tanner, in *Inductively Coupled Plasma Mass Spectrometry*, ed. A. Montaser, Wiley-VCH, 1998, ch. 8, pp. 615–679.
- 43 K. G. Heumann, S. M. Gallus, G. Rädlinger and J. Vogl, *J. Anal. At. Spectrom.*, 1998, **13**, 1001.
- 44 C. N. Maréchal, P. Télouk and F. Albarède, *Chem. Geol.*, 1999, **156**, 251–273.
- 45 P. A. Freedman, *Geochim. Cosmochim. Acta*, 2002, **66**, A245.
- 46 F. Wombacher and M. Rehkämper, *J. Anal. At. Spectrom.*, 2003, **18**, 1371–1375.
- 47 M. E. Wieser and J. B. Schwieters, *Int. J. Mass Spectrom.*, 2005, **242**, 97–115.
- 48 M. F. Thirlwall and R. Anczkiewicz, *Int. J. Mass Spectrom.*, 2004, **235**, 59–81.
- 49 D. Buhl, A. Immenhauser, G. Smeulders, L. Kabiri and D. K. Richter, *Chem. Geol.*, 2007, **244**, 715–729.
- 50 E. D. Young, E. Tonui, C. E. Manning, E. Schauble and C. Marcis, *Earth Planet. Sci. Lett.*, 2009, **288**, 524–533.
- 51 R. Chakrabarti and S. B. Jacobsen, *Earth Planet. Sci. Lett.*, 2010, **293**, 349–358.
- 52 U. Wiechert and A. N. Halliday, *Earth Planet. Sci. Lett.*, 2007, **256**, 360–371.
- 53 K. Larsen, A. Trinquier, C. Paton, M. Schiller, D. Wielandt, M. A. Ivanova, J. N. Connelly, Å. Nordlund, A. N. Krot and M. Bizzarro, *Nature Geoscience*, 2010, submitted.
- 54 G. Audi, A. H. Wapstra, C. Thibault, J. Blachot and O. Bersillon, *Nucl. Phys. A*, 2003, **729**, 3–128.
- 55 E. D. Young, A. Galy and H. Nagahara, *Geochim. Cosmochim. Acta*, 2002, **66**, 1095–1104.